ELSEVIER

Biophysical Chemistry 97 (2002) 121–128

Biophysical Chemistry

www.elsevier.com/locate/bpc

Local dynamic properties of the heme pocket in native and solvent-induced molten-globule-like states of cytochrome *c*

V. Militello[a,*], M. Leone[b], A. Cupane[b], R. Santucci[c], A. Desideri[d]

[a]*Istituto Nazionale per la Fisica della Materia and Dipartimento di Medicina Sperimentale, University of Palermo, Corso Tukory 129, 90134 Palermo, Italy*

[b]*Istituto Nazionale per la Fisica della Materia and Dipartimento di Scienze Fisiche ed Astronomiche, University of Palermo, Palermo, Italy*

[c]*Dipartimento di Medicina Sperimentale e Scienze Biochimiche, University of Rome 'Tor Vergata', Rome, Italy*

[d]*Istituto Nazionale per la Fisica della Materia and Dipartimento di Biologia, University of Rome 'Tor Vergata', Via della Ricerca Scientifica e Tecnologica, 00133 Rome, Italy*

Received 14 January 2002; received in revised form 25 February 2002; accepted 25 February 2002

Abstract

We report the Soret absorption band, down to cryogenic temperature, of native and molten-globule-like state of horse heart cytochrome *c*. The band profile is analyzed in terms of vibronic coupling of the heme normal modes to the electronic transition in the framework of the Franck–Condon approximation. From the temperature dependence of the Gaussian broadening and of the peak position, we obtain information on the 'bath' of low frequency harmonic motions of the heme group within the heme pocket. The reported data indicate that, compared to the native state, the less rigid tertiary structure of the molten globule is reflected in a higher flexibility of the heme pocket and in greater conformational disorder, allowing the transduction of large-amplitude motion of the protein to the dynamics of the heme pocket.

Keywords: Protein dynamics; Optical absorption spectroscopy; Molten-globule proteins

1. Introduction

The largely different functional properties exploited by proteins owning the same active group and the same folding arrangement indicate that not only is the three-dimensional organization of a protein important for function, but also the dynamics. Actually, structural studies have enormously influenced our view of catalysis, providing the three-dimensional pictures of active sites, but, although these time-averaged structures are very useful, they lack the information coming from the wide range of dynamics occurring in a protein. This explains why the relationship between the structural and dynamic properties of proteins in their native state, and in particular of heme-containing proteins, have been extensively inves-

*Corresponding author. Tel.: +39-091-6511243; fax: +39-091-6511914.

E-mail address: militelo@fisica.unipa.it (V. Militello), desideri@uniroma2.it (A. Desideri).

0301-4622/02/$ - see front matter
PII: S0301-4622(02)00044-3

tigated using either experimental or simulative approaches [1–9].

Less is known about the structural and dynamic properties of the so-called molten globule state, a stable intermediate state of proteins possessing a regular secondary structure, but a much less-defined tertiary arrangement [10,11]. For some proteins it has been shown that their molten globule state displays a relatively compact configuration that shows resistance to extensive proteolysis [12,13], although they also display an enhanced chain flexibility, as observed by hydrogen/deuterium exchange NMR data [14]. In this respect, an investigation comparing the dynamic properties of native and partially folded protein can give new insight into the role played by the tertiary structure in modulating protein dynamics.

Recently, the occurrence of a conformational transition of ferric cytochrome *c* dissolved in water/glycerol mixtures upon varying the amount of poly-alcohol has been shown; in particular, it was shown that upon increasing the glycerol concentration up to 99%, it is possible to stabilize a form, called G state, which is characterized by partial molten-globule character [15], since it shows spectroscopic properties similar to the acidic molten globule, or A state. The main difference between G and A states is in the spin state, since, whereas the A state is a mixed-spin form [16], the G state is predominantly a low-spin form [15]. On the other hand, in up to 70% glycerol solution the protein maintains its native conformation.

This finding gives the possibility of carrying out a comparative study of the dynamic properties of the heme pocket in cytochrome *c* in its native and molten-globule state via a line-shape investigation, as a function of temperature, of the Soret absorption band. This experimental approach arises from the fact that the optical band profile of a chromophore embedded in a matrix, such as the heme bound in a protein, undergoes spectral changes on lowering the temperature (peak frequency shift, line width narrowing and gain or loss of the integrated intensity) as a consequence of the interaction of the optical electrons with the motion of the nearby nuclei. Therefore, a detailed analysis of the line-shape as a function of temperature contains information on the dynamic properties of the complex in interactions with its environment [17–23].

The results reported indicate that the two samples display significant differences in their dynamic properties and give evidence of the role played by the protein matrix in modulating the heme pocket dynamics.

2. Materials and methods

2.1. Sample preparation

Horse heart cytochrome *c* (type VI) and glycerol were from Sigma (St. Louis, USA). Samples for optical measurements were prepared by diluting the samples into 70% v/v or 99% v/v glycerol/water solutions, at a final concentration of approximately 10 μM. Since the lyophilized protein is hardly soluble in pure glycerol, glycerol solutions (up to approx. 99.0% glycerol solution) were formed by adding a few μl of a concentrated aqueous solution of cytochrome *c* (1 mM to approximately 20 mM stock, depending on the final concentration) in pure glycerol.

2.2. Absorption measurements

Spectra in the range 500–300 nm were measured with a Cary Varian 2300 spectrophotometer. Over the whole wavelength range, the experimental conditions were: scan speed, 0.5 nm s^{-1}; integration time, 1 s; and bandwidth 0.5 nm, which corresponds to a spectral resolution of ≈ 30 cm^{-1} at 400 nm. Samples were cooled down at a rate of 1.5 K min^{-1} in a homemade optical Dewar flask equipped with optical windows and were kept at each temperature for 10 min to equilibrate. The baseline (cuvette + solvent), measured at 300 K, was subtracted from each spectrum.

2.3. Data analysis

Data were recorded at 0.5-nm intervals. The analysis of the absorption spectra was carried out using a Marquardt-type non-linear least-squares algorithm. The analytical procedure used to analyze the Soret band profiles at various temperatures has been previously reported (see [20] and refer-

ences therein), and only the principal aspects of the analysis are given here.

The absorption line shape of the Soret band results from a Franck–Condon-type of coupling of a fully allowed electronic transition of the porphyrin (from the ground to B excited states) with vibrational modes of the system. Under this hypothesis, the spectral profile can be described by the convolution of two terms:

$$F(\nu) = M\nu[L(\nu) \otimes G(\nu)] \tag{1}$$

where M is a constant proportional to the square of the electric dipole matrix element (zero-order term in the expansion of dipole moment in terms of normal vibrational coordinates).

The first term, $L(\nu)$, is a Lorentzian line-shape taking into account the electron-vibrational coupling of the so-called 'high-frequency' modes, defined as modes with a vibrational energy larger than the thermal energy, over the whole temperature range investigated ($h\nu \gg K_B T$); this implies that for these modes the electronic promotion occurs essentially from their zeroth vibrational state of the electronic ground state. In the framework of Franck–Condon approximation, $L(\nu)$ can be written as:

$$L(\nu) = \sum_{\{m_h\}} \left\{ \left[\prod_{h=1}^{N_h} \frac{e^{-S_h} S_h^{m_h}}{m_h!} \right] \times \frac{\Gamma}{\left(\nu - \nu_0 - \sum_{h=1}^{N_h} m_h \nu_h \right)^2 + \Gamma^2} \right\} \tag{2}$$

where Γ is a damping factor related to the finite lifetime of the excited state (homogeneous broadening). Eq. (2) represents a series of Lorentzian functions centered at the pure electronic transition ν_0 and at the vibronic replicas due to the coupling with N_h 'high-frequency' vibrational modes with frequency ν_h; the sum extends to the entire set of their occupation numbers $\{m_h\}$. Values of the vibronic coupling of the 'high-frequency' modes are described by the linear coupling constants S_h.

The second term in Eq. (1), $G(\nu)$, takes into account the coupling of the electronic transition with the bath of 'low-frequency' vibrational modes, i.e. those vibrational modes characterized by vibrational energy lower than the thermal energy ($h\nu \ll K_B T$). Due to the thermal dependence of the occupation numbers of their highest vibrational states within the electronic ground state, the coupling with low-frequency modes gives rise to a temperature-dependent broadening of the Lorentzian profile that can be written as:

$$G(\nu) = \sigma(T)^{-1} \exp\left[-\frac{\nu^2}{2\sigma^2(T)} \right] \tag{3}$$

Within the framework of the harmonic approximation and considering the 'low-frequency' bath as an ensemble of N degenerate harmonic oscillators (Einstein approximation), the temperature dependence of the Gaussian width can be expressed as:

$$\sigma^2(T) = N \; S\langle\nu\rangle^2 \coth\left[\frac{h\langle\nu\rangle}{2k_B T} \right] + \sigma_{in}^2 \tag{4}$$

where k_B is the Boltzmann constant, N, S and $\langle\nu\rangle$ are the total number, the effective linear coupling constant and the frequency of the 'low-frequency' bath, respectively. In Eq. (4), the σ_{in} term accounts for temperature-independent inhomogeneous broadening.

In the presence of quadratic coupling, the parameter ν_0 also becomes temperature dependent [20]; within the harmonic approximation its thermal behavior can be expressed as:

$$\nu_0(T) = \nu_{00} - \frac{1}{4} N\langle\nu\rangle(1-R) \coth\left[\frac{h\langle\nu\rangle}{2k_B T} \right] + C \tag{5}$$

where R is an effective quadratic coupling constant, ν_{00} is the frequency of the purely electronic ($0 \rightarrow 0$) transition, and C accounts for other temperature-independent contributions to the peak position of the band.

According to the above-reported analytical procedure taking into account the line-shape of the optical bands, we perform a first non-prejudiced fitting of the low-temperature Soret spectra of the samples studied in terms of Eqs. (1)–(3). This allows extraction of 'structural' parameters, such as the values of the homogeneous broadening, Γ, related to the finite lifetime of the excited elec-

tronic states, and of the coupling constants, S_h, relative to the 'high-frequency' Franck–Condon active vibrational modes. For the data reported here, we consider the coupling with seven 'high-frequency' Franck–Condon active vibrational modes, fixed at 348, 569, 681, 1372, 1503, 1583 and 1636 cm^{-1}, respectively. These values refer to the most intense peaks found by resonance Raman spectroscopy of the Fe^{3+} derivative of cytochrome *c*, under excitation within the Soret band [24]. The value of the Γ parameter worked out from this fitting procedure is quite large, being approximately 550 cm^{-1} for both native and molten-globule cytochrome *c*, and very close to the value found by Schomacker et al. [24]. From this first analysis of the low-temperature spectra, we can appreciate S_h values relative to the coupling with the in-plane A_{1g} modes at 681 and 1372 cm^{-1}, that were found as 0.15 ± 0.05 and 0.10 ± 0.05, respectively, both for cyt-N and for cyt-G samples, whereas for the remaining modes, S_h values less then 0.05 (i.e within the experimental error) were obtained. We wish to stress that, in view of the large value of the Γ parameter, S_h values must be considered as mean values. The overall fitting procedure for the Soret band must also be considered as a function of temperature. In order to avoid fitting ambiguities at high temperatures, arising from broadening of the spectral profiles and from the lack of a clearly resolvable vibronic structure, we neglect the coupling with all 'high-frequency' vibrational modes except the two A_{1g} modes at 681 and 1372 cm^{-1}. Moreover, the S_h coupling constants of these two modes and the Γ parameter were fixed at their low-temperature values when the analysis of the spectra is outlined over the whole temperature range investigated.

The procedure outlined above allows singling out of the different contributions to the overall bandwidth observed, including the homogeneous broadening due to non-radiative decay of the excited electronic state (Γ parameter), the coupling with high-frequency nuclear vibrations responsible for the vibronic structure of the spectra (S_h parameters) and the Gaussian broadening due to the coupling with a bath of low-frequency motion (temperature dependent) and due to the conformational heterogeneity (σ_{in} parameter) [17–23].

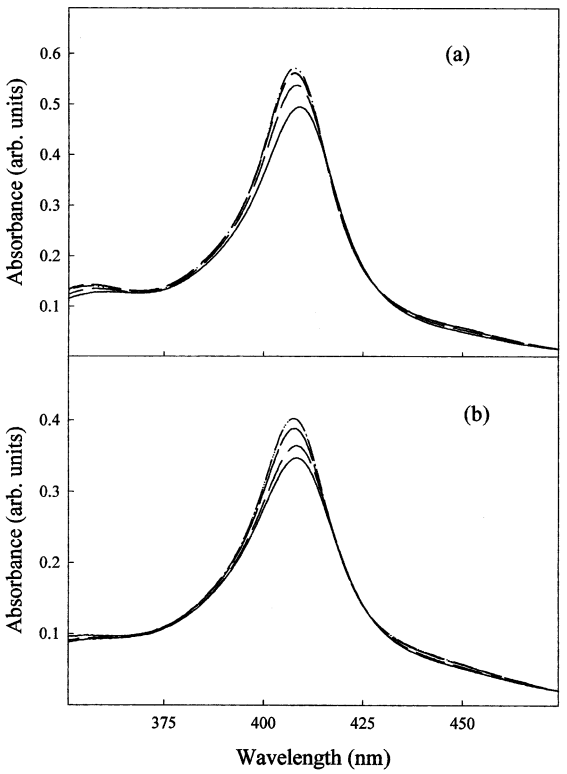

Fig. 1. The Soret spectra at various temperatures for (a) cyt-N and (b) cyt-G samples: (_____) $T=300$ K; (__ __) $T=220$ K; (_ _ _) $T=140$ K; and (_··_··) $T=15$ K.

3. Results and discussion

Fig. 1 shows Soret absorption spectra of the native (cyt-N) and molten globule (cyt-G) state of horse heart cytochrome *c*, as a function of temperature. For both samples, the absorption spectra consist of a broad main band, centered at approximately 410 nm and ascribed to an *x–y*-polarized $\pi-\pi^*$ transition of the tetragonally symmetric heme chromophore [25]; in the low wavelength region, a spectral contribution attributed to a different $\pi-\pi^*$ transition (N band) is also observed. The shoulder at approximately 440 nm, particularly evident at low temperature, is attributed to a spin-allowed transition in analogy with other low-spin Fe(III) complexes, such as

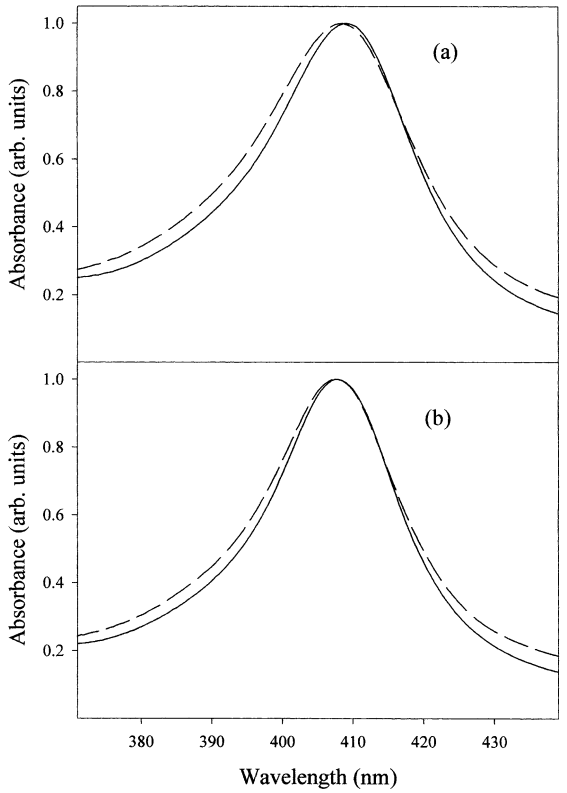

Fig. 2. The Soret spectra, normalized to the maximum intensity, at (a) 300 and (b) 15 K: continuous lines, cyt-N; dashed lines, cyt-G.

cyanomet derivatives of heme proteins [26]. The raw data show that the Soret band of cyt-G is very similar to that of cyt-N, excluding a slight but significant difference in the bandwidth, as shown in Fig. 2, where the normalized spectra of the two samples are reported for low and high temperatures.

The overall band profile can be deconvoluted in terms of Eqs. (1)–(3) for each temperature, taking into account the contribution of the main Soret band, as well as two Gaussian components, centered at 29 000 and 22 600 cm^{-1}, that account for the spectral contributions of the N band and of the shoulder on the red side of the spectra, respectively. Fig. 3 shows the deconvolution of the low-temperature spectra according to the fitting procedure outlined in Section 2.3, the relative parameters being reported in Table 1. We note that the quality

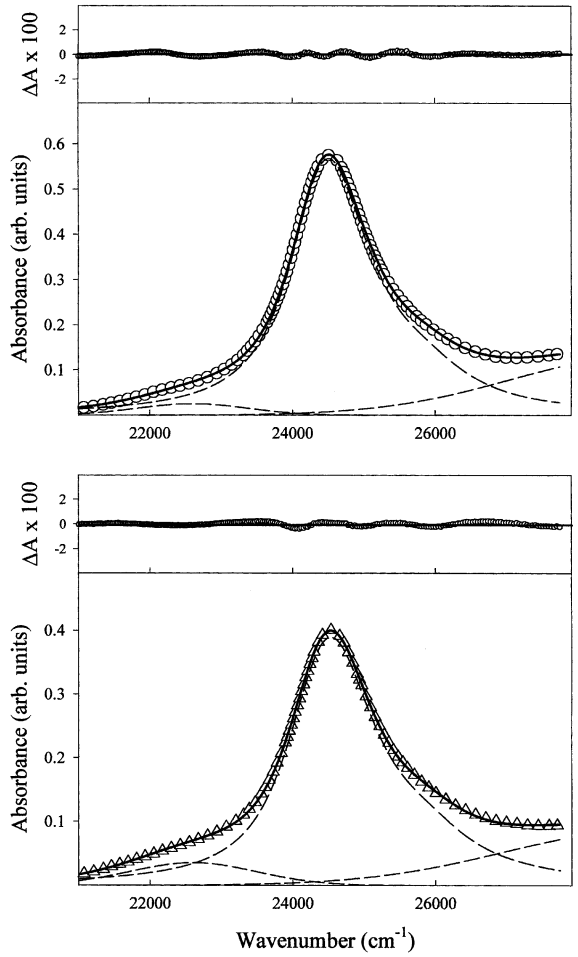

Fig. 3. Deconvolution of the low-temperature spectra of cyt-N (upper panels, circles) and of cyt-G samples (lower panels, triangles). For the sake of clarity, not all the experimental points are reported. Dashed lines represent the spectral contribution of the main Soret band in terms of Eq. (2), of the N band (blue side region) and of the low-frequency band (red side region, see text); the continuous lines represent the overall profiles synthesized. For each deconvolution, the residuals are also reported in the upper panels.

Table 1
Values of the homogeneous width, Γ, and linear coupling constant, *S*, obtained from the analysis of the Soret band in terms of Eqs. (1) and (2)

	Γ	S_{685}	S_{1372}
Cyt-N	550 ± 10	0.10 ± 0.05	0.15 ± 0.05
Cyt-G	550 ± 10	0.10 ± 0.05	0.14 ± 0.05

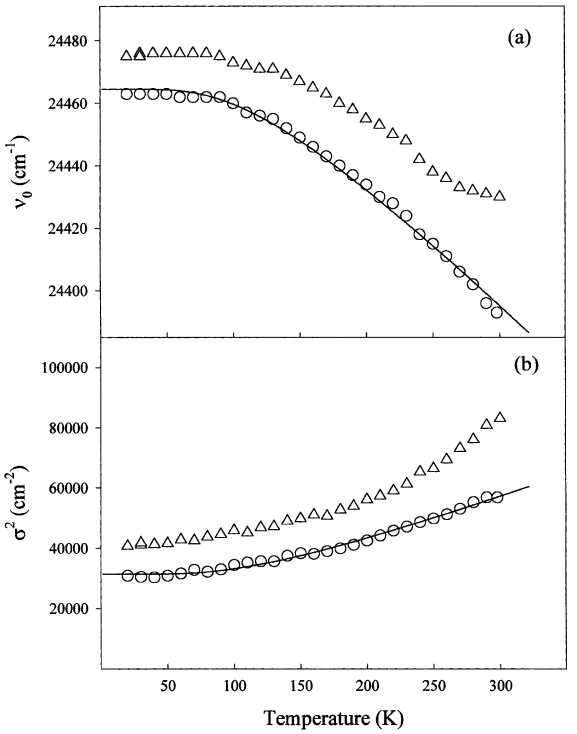

Fig. 4. (a) ν_0 and (b) σ^2 thermal behavior obtained by the deconvolution of the Soret bands for cyt-N (circles) and cyt-G (triangles). Continuous lines represent the fitting for cyt-N data in terms of Eqs. (5) and (4), respectively.

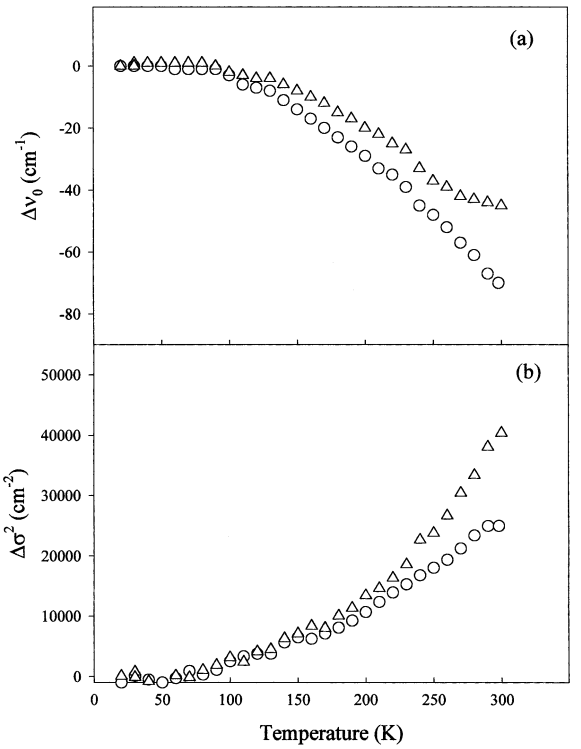

Fig. 5. $\Delta\nu_0$ and $\Delta\sigma^2$ values (see text) as a function of temperature. Symbols as in Fig. 4.

of the fitting is excellent, as demonstrated by the residuals reported, and that the same, or better quality, is obtained for each temperature.

The data reported in Table 1 show very similar values of the parameters Γ and S_h for the two samples, in agreement with the oxidized state of the iron (as suggested by Santucci et al. [15]); this fact suggests that the porphyrin moiety in the G state of cytochrome *c* is not subject to any relevant in-plane structural distortion when compared to its condition in the N state.

Conversely, the two samples display significant differences in their dynamic properties, as evidenced by the thermal behavior of the Gaussian width, σ^2, and of the peak frequency of the band, ν_0, reported in Fig. 4. A first inspection of the data shows that the harmonic behavior predicted by Eqs. (4) and (5) for $\sigma^2(T)$ and $\nu_0(T)$, respectively, is obeyed over the whole temperature range only by the cyt-N sample (see continuous lines in Fig. 4). The parameters obtained for cyt-N are reported in Table 2. To demonstrate the temperature dependence of the broadening of the bands,

Table 2
Values of the parameters obtained by fitting the $\sigma^2(T)$ and $\nu_0(T)$ thermal behavior for cyt-N in terms of Eqs. (4) and (5), respectively

	$N{\cdot}S$	$\langle\nu\rangle$ (cm^{-1})	σ_{in} (cm^{-1})	$\nu_{00}+C$ (cm^{-1})	R[a]
Cyt-N	0.48 ± 0.04	245 ± 10	55 ± 4	24.542 ± 8	0.975 ± 0.006

[a] The R values are obtained by assuming the coupling with $N=50$ low-frequency modes.

we report in Fig. 5 the quantities (a) $\nu_0(T) - \nu_0(T=0)$ and (b) $\Delta\sigma^2 = \sigma^2(T) - \sigma^2(T=0)$.

Figs. 4 and 5 suggest that the native form of cytochrome *c* keeps the heme complex in a very rigid and 'solid-like' structure, even at room temperature; this is demonstrated by the harmonic behavior found for the local dynamics of the active site. This behavior is not found in other heme-proteins, such as hemoglobin or myoglobin [19,23], where substate interconversion of the protein matrix [26–28] needed for their functional behavior contributes large anharmonic terms to the local dynamics of the heme pocket.

Finally, the σ^2 value at low temperature (see Fig. 4) is greater for cyt-G than for cyt-N, indicating that the molten-globule-like state is characterized by greater conformational heterogeneity.

These results indicate the presence of less rigid constraints in cyt-G: we suggest that the overall protein tertiary structure changes, evidenced by the circular dichroism (CD) data in the aromatic region at approximately 280 nm [15], induce a conformational rearrangement of the heme pocket that allows dynamic coupling of the heme with a less rigid environment and favors the transduction of anharmonic motion to the heme complex. Disruption of the Fe(III)–Met 80 bond and the subsequent binding of an endogenous histidine to the heme iron, as suggested by Santucci et al. [15], may also contribute to the above effect.

4. Conclusions

Analysis of thermal behavior of the optical spectra of cyt-N and cyt-G has allowed us to investigate the local structural and dynamic properties of the active site (heme pocket) of the native and molten-globule states of this protein. For both samples, the heme complex displays similar structural properties, as described by the Γ and S_h parameters that are related to the electronic states of the macrocycle and to their interaction with high-frequency vibrations, respectively. On the other hand, the dynamics of the active site, as monitored by the temperature dependence of the electronic absorption of the heme complex, displays remarkable differences in the native and molten-globule states. In fact, the thermal behavior of the ν_0 and σ^2 parameters for cyt-N follows a harmonic trend over the whole temperature range investigated, whereas, for cyt-G, deviations from harmonicity are evident. This fact suggests that the loose matrix of the molten globule is able to transmit within the heme pocket the jumping between different conformational substates, which characterize the high temperature 'liquid-like' state of the protein, causing high non-harmonic contributions to the local dynamics.

This result is the first evidence of perturbed local dynamics monitored at the level of the heme complex between native and molten-globule states of cytochrome *c* and underlines the important role played by the protein matrix in modulating local dynamics.

Acknowledgments

The technical help of Mr G. Lapis of the cryogenic laboratory in Palermo is acknowledged. This work was partly supported by Ministero Italiano dell'Università e della Ricerca Scientifica e Tecnologica (MURST), project Cofin 2000.

References

[1] R.H. Austin, K. Beeson, L. Eisenstein, H. Frauenfelder, I.C. Gunsalus, V.P. Marshall, Dynamics of carbon monoxide binding to heme proteins, Science 181 (1973) 541–543.

[2] D.A. Case, M. Karplus, Dynamics of ligand binding to heme proteins, J. Mol. Biol. 132 (1979) 343–368.

[3] P.J. Steinbach, A. Ansari, J. Berendzen, et al., Ligand binding to heme proteins: connection between dynamics and function, Biochemistry 30 (1991) 3988–4001.

[4] E.E. Di Iorio, U.R. Hiltpold, D. Filipovich, et al., Protein dynamics. Comparative investigation on heme-protein with different physiological roles, Biophys. J. 59 (1991) 742–754.

[5] A. Cupane, M. Leone, E. Vitrano, et al., Structure–dynamics–function relationships in Asian elephant (*Elephas maximus*) myoglobin. An optical and flash-photolysis study on functionally important motions, Biophys. J. 65 (1993) 2461–2472.

[6] G. Smulevich, S. Hu, R. Rodgers, D.B. Goodin, K.M. Smith, T.G. Spiro, Heme–protein interactions in cytochrome *c* peroxidase revealed site-directed mutagenesis and resonance Raman spectra of isotopically labeled hemes, Biospectroscopy 2 (1996) 365–376.

[7] M. Leone, A. Cupane, V. Militello, M.E. Stroppolo, A. Desideri, Fourier-transform infrared analysis of the inter-

action of azide with the active site of oxidized and reduced bovine Cu, Zn superoxide dismutase, Biochemistry 37 (1998) 4459–4464.
[8] M. Falconi, A. Desideri, A. Cupane, et al., Structural and dynamic properties of the homodimeric hemoglobin from *Scapharca inaequivalvis* Thr72→Ile mutant: molecular dynamics simulation, low-temperature visible absorption spectroscopy and resonance Raman spectroscopy studies, Biophys. J. 75 (1998) 2489–2503.
[9] N. Engler, A. Ostermann, A. Gassmann, et al., Protein dynamics in an intermediate state of myoglobin: optical absorption, resonance Raman spectroscopy and X-ray structure analysis, Biophys. J. 78 (2000) 2061–2092.
[10] K. Kuwajiama, The molten globule state as a clue for understanding the folding and co-operativity of globular-protein structure, Proteins 6 (1986) 87–103.
[11] O.B. Ptitsyn, Molten globule and protein folding, Adv. Protein Chem. 47 (1995) 83–229.
[12] P. Polverino de Laureto, V. De Filippis, M. Di Bello, M. Zambonin, A. Fontana, Probing the molten globule state of alpha-lactalbumin by limited proteolysis, Biochemistry 34 (1995) 12596–12604.
[13] A. Fontana, P. Polverino de Laureto, V. De Filippis, E. Scaramella, M. Zambonin, Probing the partly folded states of proteins by limited proteolysis, Folding Design 2 (1997) R17–R26.
[14] C.L. Chyan, C. Wormald, C.M. Dobson, P.A. Evans, J. Baum, Structure and stability of the molten globule state of guinea-pig alpha-lactalbumin: a hydrogen exchange study, Biochemistry 32 (1993) 1707–1718.
[15] R. Santucci, F. Polizio, A. Desideri, Formation of a molten-globule-like state of cytochrome *c* induced by high concentrations of glycerol, Biochimie 81 (1999) 745–751.
[16] Y. Goto, L.J. Calciano, A.L. Fink, Acid-induced folding of proteins, Proc. Natl. Acad. Sci. USA 87 (1990) 573–577.
[17] J.J. Markham, Interactions of normal modes with electron traps, Rev. Mod. Phys. 3 (1959) 956–989.
[18] K.T. Schomacker, P.M. Champion, Investigations of spectral broadening mechanisms in biomolecules, J. Chem. Phys. 84 (1986) 5314–5325.
[19] M. Leone, A. Cupane, V. Militello, L. Cordone, Thermal broadening of Soret band in heme complexes and in heme-proteins: role of the iron dynamics, Eur. Biophys. J. 23 (1994) 349–352.
[20] A. Cupane, M. Leone, E. Vitrano, L. Cordone, Low-temperature optical absorption spectroscopy: an approach to the study of stereodynamic properties of heme proteins, Eur. Biophys. J. 23 (1995) 385–398.
[21] B. Melchers, E.W. Knapp, F. Parak, L. Cordone, A. Cupane, M. Leone, Structural fluctuations of myoglobin derived from normal-modes, Mossbauer, Raman and absorption spectroscopy, Biophys. J. 70 (1996) 2092–2099.
[22] R. Schweitzer-Stenner, A. Cupane, M. Leone, C. Lemke, J. Schott, W. Dreybrodt, Anharmonic protein motions and heme deformations in myoglobin cyanide probed by absorption and resonance Raman spectroscopy, J. Phys. Chem. 104 (2000) 4754–4764.
[23] V. Sanfratello, A. Boffi, A. Cupane, M. Leone, Heme symmetry, vibronic structure and dynamics in heme proteins: ferrous nicotinate horse myoglobin and soybean leghemoglobin, Biopolymers (Biospectroscopy) 57 (2000) 291–305.
[24] K.T. Schomacker, O. Bangcharoenpaurpong, P.M. Champion, Investigation of the Stokes and anti-Stokes resonance Raman scattering of cytochrome *c*, J. Chem. Phys. 80 (1984) 4701–4717.
[25] M.W. Makinen, A.K. Churg, Structural and analytical aspects of the electronic spectra of heme proteins, in: A.B.P. Lever, H.B. Gray (Eds.), Iron Porphyrins, 1983, p. 141.
[26] M. Leone, A. Cupane, L. Cordone, Low-temperature optical spectroscopy of low-spin ferric heme proteins, Eur. Biophys. J. 24 (1996) 117–124.
[27] H. Frauenfelder, F. Parak, R.D. Young, Conformational substates in proteins, Annu. Rev. Biophys. Biophys. Chem. 17 (1988) 451–479.
[28] F. Parak, G.U. Nienhaus, Glass-like behavior of proteins as seen by Mossbauer spectroscopy, Non-Cryst. Solids 131–133 (1991) 362–368.